Geochemical Perspectives Letters

Enrichment mechanism of trace elements in pyrite under methane seepage

X. Miao[1], X. Feng[1,2*], J. Li[2], X. Liu[1,2], J. Liang[3,4], J. Feng[3,4], Q. Xiao[1], X. Dan[1], J. Wei[3,4*]

https://doi.org/10.7185/geochemlet.2211

Abstract

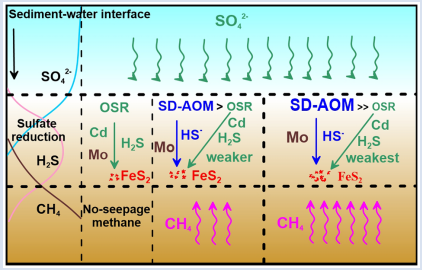

Authigenic pyrite is an important recorder for methane seepage. During methane seepage, the sulfur and iron isotopic composition of pyrite will change, allowing it to be used as an indicator to identify methane seepage. However, the dissimilar behaviour of trace elements in authigenic pyrite during methane seepage remain unclear. To provide insights, we used pyrite samples from the 'Haima' seep locality to determine differences in trace element contents in pyrite obtained from the sulfate-methane transition zone (SMTZ) and that from normal (non-seepage) sedimentary environments. In the SMTZ, the content of cadmium (Cd) related to the organoclastic sulfate reduction in pyrite was low, while the molybdenum (Mo) content, which is highly sensitive to redox environments, was high. This discrepancy can be explained by the fact that sulfate ions (SO_4^{2-}) in the SMTZ were preferentially consumed by sulfate driven anaerobic oxidation of methane (SD-AOM), which inhibited organoclastic sulfate reduction and decreased the trace metals derived from organic matter in pore water. Simultaneously, intense SD-AOM produced more hydrogen sulfide (H_2S), which was more conducive to Mo removal from pore water, and then more Mo adsorption onto pyrite. Further analysis shows that the Mo/Cd ratio of pyrite in the SMTZ (average value of 82.08) is significantly higher than that of the non-SMTZ (average value of 16.02). We believe that the Mo/Cd ratio has great potential to indicate methane seepage, and thus provides a new indicator for methane seepage research.

Received 8 November 2021 | Accepted 27 February 2022 | Published 1 April 2022

Introduction

Authigenic pyrite is considered to be the most important sulfide mineral because it is more stable than other iron sulfides and is the main sink of sulfur (Berner, 1984). Its formation is often related to organoclastic sulfate reduction (OSR), using organic matter and seawater sulfate as substrate and yielding hydrogen sulfide (H_2S) (Berner, 1984). However, OSR is different (*e.g.*, reaction rates) in various sedimentary environments (Berner, 1978). This will eventually lead to corresponding changes in the morphology and geochemical characteristics of pyrite (Berner, 1978, 1984; Huerta-Diaz and Morse, 1992; Wilkin *et al.*, 1996). In recent years, many indicators have been used to study sedimentary environment evolution, such as the sulfur and iron isotopic compositions of pyrite (Lin *et al.*, 2016), the grain size of framboidal pyrite (Wilkin *et al.*, 1996), and iron speciation (Slotznick *et al.*, 2018). Trace elements can also adsorb onto pyrite, an important sink in many geochemical cycles that has great potential for reconstructing palaeoenvironments (Morse and Luther, 1999; Berner *et al.*, 2013; Mukherjee and Large, 2020; Large *et al.*, 2022). Initially, research on trace elements in pyrite mainly focused on defining ore genetic types, determining the source of ore forming materials, and inverting the evolution of ore forming fluids (Clark *et al.*, 2004; Large *et al.*, 2009; Ulrich *et al.*, 2011). As research has advanced, scientists have found that the composition of trace elements in diagenetic pyrite is greatly affected by the geochemical characteristics of pore water in the sediments (Huerta-Diaz and Morse, 1992; Berner *et al.*, 2013; Large *et al.*, 2014, 2022). When the concentration of H_2S in the environment increases, those of redox sensitive elements (such as Mo) in pyrite will also increase (Huerta-Diaz and Morse, 1992; Berner *et al.*, 2013). Therefore, trace elements in diagenetic pyrite within sediments can be used to record the geochemical information of original sedimentary environments and have great potential for palaeoenvironmental reconstruction.

However, there are some unique sedimentary environments where additional sources of H_2S play an important role in pyrite formation, such as hydrothermal environments (Large *et al.*, 2014) and oil seepage areas (Steadman *et al.*, 2021). Cold seep environments are also important sedimentary environments for the dissociation of seabed natural gas hydrate. Both methane released from cold seeps and the sulfate released from seawater undergo sulfate driven anaerobic oxidation of methane

1. Key Laboratory of Submarine Geosciences and Prospecting Technology, College of Marine Geosciences, Ocean University of China, Qingdao 266100, China
2. Pilot National Laboratory for Marine Science and Technology, Qingdao 266037, China
3. MLR Key Laboratory of Marine Mineral Resources, Guangzhou Marine Geological Survey, Guangzhou 510075, China
4. Southern Marine Science and Engineering Guangdong Laboratory (Guangzhou), Guangzhou 511458, China
* Corresponding author (email: fengxiuli@ouc.edu.cn; weijiangong007@163.com)

(SD-AOM) in the sulfate-methane transition zone (SMTZ) (Boetius *et al.*, 2000). This releases a large amount of H_2S and provides the constituents necessary to form pyrite (Lin *et al.*, 2016). Thus, pyrite formation in normal marine sedimentary environments and cold seep environments is controlled by different geochemical processes (OSR *vs.* SD-AOM). Based on previous studies of trace elements in authigenic carbonate and sediments in methane seepage, we found a remarkable dependency: when Mo is enriched, Cd, Ni, Cu, and Zn are not enriched (Sato *et al.*, 2012; Chen *et al.*, 2016). We speculate that pyrite generated in methane seepage environments and in normal marine sedimentary environments should have obvious differences in their geochemical elemental composition.

To test this hypothesis, here we used pyrite samples from the Haima seep sedimentary area to compare the trace element contents in pyrite obtained from the SMTZ and in pyrite obtained from normal (non-seepage) sedimentary environments. This provides a new perspective for identifying methane seepage and provides a new reference for discussing the relationship between pyrite elements and sedimentary environments.

Materials and Methods

The Q6 core was taken by the Guangzhou Marine Geological Survey in 2019 using the R/V Haiyang-6 (Fig. 1a). Based on previous geochemical analysis results (Miao *et al.*, 2021a,b), we identified several palaeo-methane seeps using TS/TOC, sulfur isotopes, and iron speciation (Fig. 1b). To test their elemental compositions, we selected pyrite from different Q6 layers and then conducted laser ablation inductively coupled plasma mass spectrometry (LA-ICP-MS) to analyse pyrite obtained from the methane seepage environments and from normal sedimentary environments. For more detailed information, please refer to the Supplementary Information.

Results

Trace element contents of the pyrites are shown in Figure 2. In Q6, the Cd content of pyrite taken from the methane seepage was lower than that of pyrite from the normal sedimentary environment. The corresponding average value (and its range) was 1.02 ppm (0.03–7.54 ppm). In a normal sedimentary environment, the average Cd contents were higher, with the corresponding average value (and its range) being 8.5 ppm (0.1–99.5 ppm). At the same time, the Mo content was significantly higher in pyrite from the methane seepage, with the average value (and its range) equal to 61.9 ppm (3.9–350.5 ppm), while, in a normal sedimentary environment, the Mo content was significantly lower, with the average value (and its range) equal to 28.1 ppm (0.1–84.5 ppm). It is shown that the Mo/Cd ratios of pyrite in the methane seepage are mostly above the line of Mo/Cd = 16.02, whereas they lie below this line for pyrites in the non-methane seepage (Fig. S-5).

There is little difference in trace element contents of As, Ni, Cu and Zn in pyrite between the methane seepages (406.0 ppm, 29.2–3396.0 ppm; 36.3 ppm, 0.5–222.4 ppm; 18.9 ppm, 0.1–103.1 ppm; 57.4 ppm, 8.6–228.2 ppm, respectively) and the normal sedimentary environment (243.8 ppm, 30.7–759.0 ppm; 37.8 ppm, 1.7–210.0 ppm; 21. 9 ppm, 2.8–78.3 ppm; 67.7 ppm, 1.0–205.1 ppm, respectively).

Discussion

Geochemical composition of trace elements in pyrite: methane vs. non-methane seepage. During early diagenesis, trace elements are captured by metastable substances in the sediment (such as labile organic matter and metastable precursors of Fe and Mn oxides). Thus, the remineralisation of labile organic matter and reductive dissolution of Fe and Mn oxides were the primary sources of trace elements in pore water in the marine sediment (Smrzka *et al.*, 2019, 2020). The Cd is mainly derived from the remineralisation of labile organic matter. The Mo is mainly derived from reductive dissolution of Fe and Mn oxides, and will be fixed into the sediment when H_2S exists (Smrzka *et al.*, 2019, 2020). In analysing the trace elements in the diagenetic pyrite, it was found that the content of Cd in pyrite generated during methane seepage was low, while the content of Mo was high (Fig. 2). This may be controlled by different biogeochemical processes for pyrite formation. In non-seepage, the formation

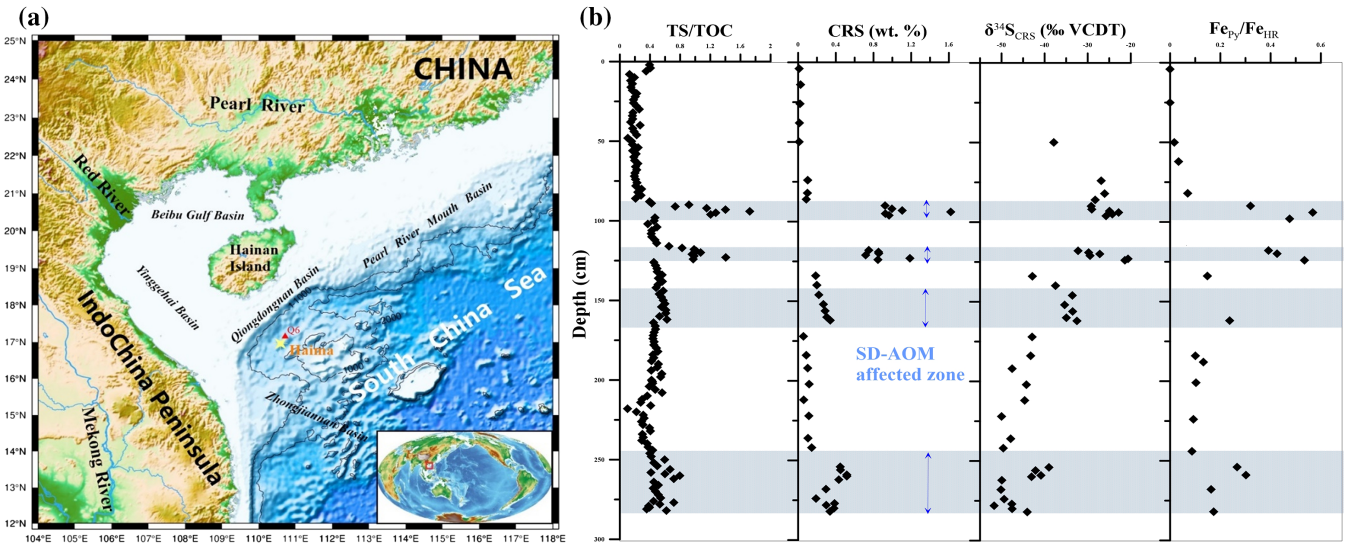

Figure 1 **(a)** Map showing the study region; the Q6 core located in the Qiongdongnan Basin of the SCS (modified from Miao *et al.*, 2021a,b). **(b)** Down core variations of TS/TOC, CRS, $\delta^{34}S_{CRS}$, and Fe_{Py}/Fe_{HR} in sediments (based on Miao *et al.*, 2021b). The blue horizontal bars indicate methane seepage (based on Miao *et al.*, 2021a,b). TS/TOC = total sulfur/total organic carbon; CRS = chromium reducible sulfur; $\delta^{34}S_{CRS}$ = sulfur isotope of chromium reducible sulfur; Fe_{py} = pyrite Fe; Fe_{HR} = highly reactive Fe.

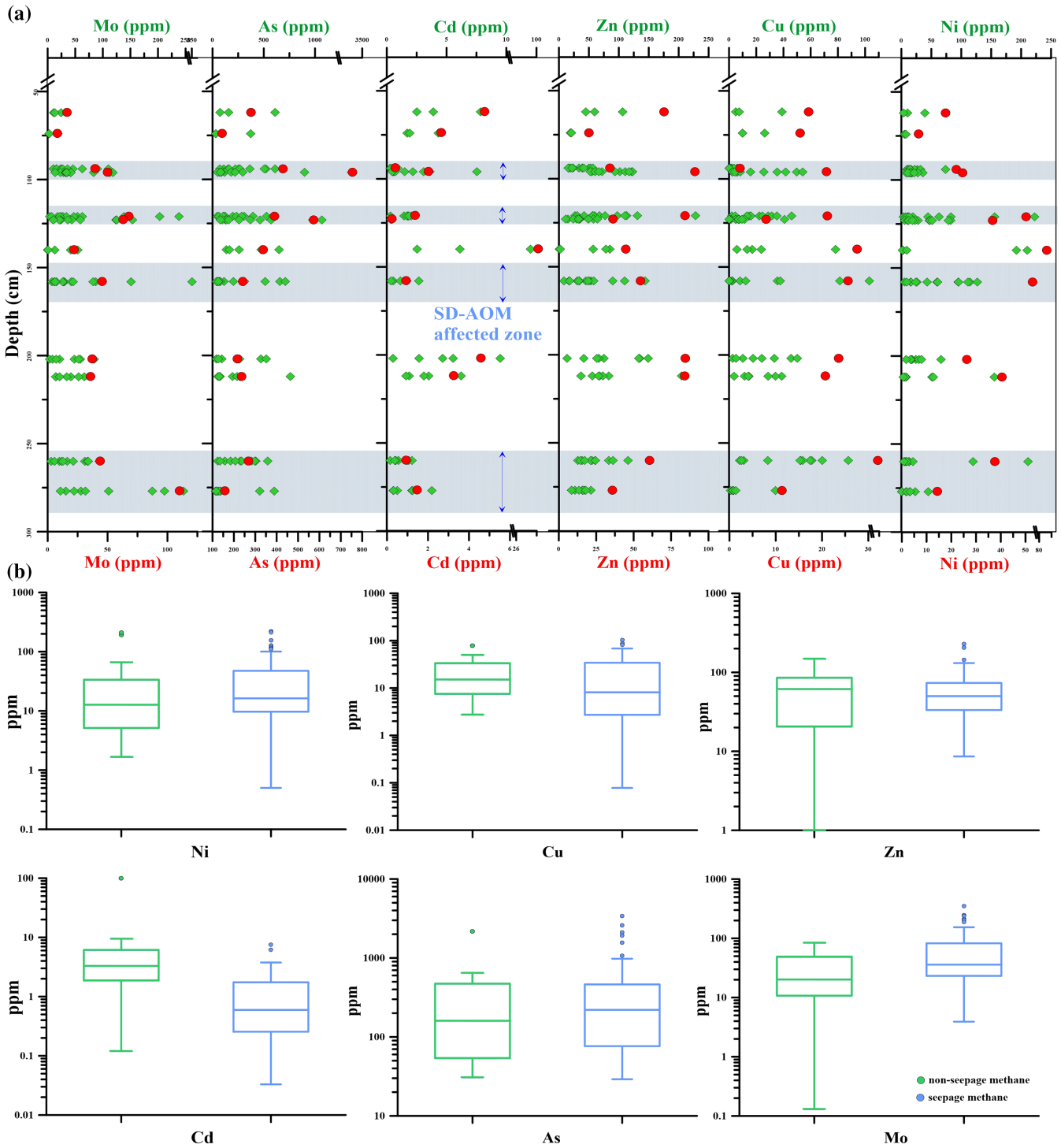

Figure 2 **(a)** Down core variations of the trace element contents (Cd, Ni, Cu, Zn, As, and Mo) in pyrite samples. The grey shaded bars indicate methane seeps; each green circle represents a single pyrite analysis; each red circle represents the average pyrite analysis. **(b)** Box plots of the average values of Ni, Cu, Zn, Cd, As, and Mo contents in pyrites.

of pyrite is mainly controlled by OSR (Berner, 1984), while SD-AOM plays a leading role in methane seepage (Lin *et al.*, 2016).

SD-AOM and OSR have significantly different influences on the distribution and behaviour of trace elements: (1) methane itself does not carry trace elements, while the organic matter contains trace elements such as Cd (Smrzka *et al.*, 2019, 2020); (2) the concentration of dissolved sulfide produced by SD-AOM is higher than that produced by OSR, which changes the behaviour of some trace elements, such as Mo (Smrzka *et al.*, 2019, 2020). These processes may eventually change the corresponding elements in pyrite. In non-seepage sedimentary environments, the OSR re-released the absorbed trace elements into the pore water during early diagenesis (Berner *et al.*, 2013; Smrzka *et al.*, 2019, 2020), which increased the content of Cd related to organics and affected their contents in pyrite. On the contrary, in the methane seepage, large amounts of methane gas generated by hydrate dissociation led to sulfate reduction (Lin *et al.*, 2016). It has been previously shown that the sulfate reduction rate in methane seeps can be several orders of

magnitude higher than that in normal marine sedimentary environments (Aharon and Fu, 2000). In addition, SD-AOM consumes less energy and is more likely to react with sulfate (Dickens, 2001). Therefore, we believe that SD-AOM first consumes a large amount of sulfate, which inhibits OSR. This process also delays the release of the absorbed trace elements from organics, which results in the lower Cd contents in the pore water. Moreover, methane itself does not carry trace elements (Smrzka *et al.*, 2020). SD-AOM should not participate directly in trace element cycling because none of the compounds involved in the reaction are trace element carriers (Smrzka *et al.*, 2019, 2020). Thus, their dissociation does not affect trace element contents in the pore water. Meanwhile, under methane seepage, the source of the trace metals in pore water is the reductive dissolution of Fe and Mn oxides. These reactions are typically unrelated to the organic matter present in the same system (Smrzka *et al.*, 2019, 2020). Thus, organic matter Cd contents were lower in the pyrite produced under methane seepage than in that produced under a normal sedimentary environment.

In the normal marine sedimentary environment, H_2S production is limited (Lin *et al.*, 2016) due to OSR being relatively slow. However, SD-AOM can accelerate sulfate reduction, yielding more dissolved sulfide, which leads to sulfide reduction in that local micro-environment (Chen *et al.*, 2016; Lin *et al.*, 2016). On the one hand, this sulfidic environment will accelerate the dissolution of Fe and Mn oxides and release more Mo into the pore water (Eroglu *et al.*, 2020). On the other hand, due to the high H_2S content, Mo will be removed from the pore water onto pyrite more efficiently (Smrzka *et al.*, 2020). Our previous work showed that the iron (oxy) hydroxides contents were very low in the SMTZ of Q6, which indicates their substantial dissolution (Miao *et al.*, 2021b). In addition, enrichment factors of Mo are positively correlated with Fe/Al ($R^2 = 0.24$), and R^2 can even exceed 0.9 at 90–98 cm ($R^2 = 0.97$) and 118–124 cm ($R^2 = 0.97$) depths, indicating that the reductive dissolution of Fe and Mn oxides plays an important role in the enrichment of Mo (Fig. S-6; Miao *et al.*, 2021a). All these results proved that the Mo enrichment in the pyrite under the methane seepage was mainly affected by SD-AOM. However, OSR does not disappear in the SMTZ. We found that the correlations between Fe_{Py} and TOC in the SMTZ are poor ($R^2 = 0.12$; Fig. S-7). This indicates that the distribution and importance of OSR-derived pyrite in methane-rich, but organic poor, sediments is limited.

In addition, the Ni, Cu, and Zn contents of pyrite in the two environments were not significantly different (Fig. 2). This may be because, of these and similar elements, Cd is the most sensitive to organic matter, and its content in sediment pore water is strongly affected by the presence of organic matter (Smrzka *et al.*, 2019, 2020). However, Ni, Cu, Zn, and other elements may combine with H_2S to different degrees to transform the corresponding sulfides into pyrite (Morse and Luther, 1999). In contrast, Huerta-Diaz and Morse (1992) found that cadmium was largely unaffected by the presence of sulfides in the pore water. Therefore, we believe that Mo/Cd ratios in diagenetic pyrite can indicate the presence of methane seeps. In Figure S-4, this conclusion is confirmed. The Mo/Cd ratio of pyrite in methane seepage is significantly higher than that in non-methane seepage (Mo/Cd > 16.02). However, no similar phenomenon was found for other elements (Fig. S-5).

Trace elements of pyrite indicate methane seepage. To further verify the effectiveness of this indicator, the Mo/Cd ratios were compared and analysed alongside the indicators used to represent methane seepage. It was found that the Mo/Cd ratios of pyrite increased with increasing TS/TOC, $\delta^{34}S_{CRS}$, and Fe_{Py}/Fe_T (Fig. 3). In non-methane seepage, Mo/Cd, TS/TOC, $\delta^{34}S_{CRS}$, and Fe_{Py}/Fe_T are located in the low value region. On the contrary, these proxies are in the high value area in methane seepage. This indicates that SD-AOM does have a great influence on the Mo/Cd ratio of pyrite. It is indicated that, compared with normal marine environment, intense methane activity can not only accelerate pyrite formation and reduce sulfur isotope fractionation, but also change the surrounding pore water environment (inhibiting OSR and changing the redox environment). Moreover, we found that the Mo/Cd ratio of pyrite at 90–124 cm depth is higher than those at 144–162 cm and 254–282 cm depths, and corresponds to a higher TS/TOC ratio and other indicators (Fig. 3). This is inferred to be related to the intensity of methane seepage. At 90–124 cm depth, the TS/TOC ratios and $\delta^{34}S_{CRS}$ values are higher (Figs. 1 and 3), indicating a higher pyrite content and faster sulfate reduction rate (Miao *et al.*, 2021b), respectively. Meanwhile, iron composition data show that the pore water environment in this formation is more inclined to euxinic environments (Fig. S-8, Slotznick *et al.*, 2018). This phenomena indicates that the methane seepage is most intensive in this layer, which further inhibits OSR. This is followed by a further reduction in Cd content in the pore water. The Cd content of pyrite in the 90–124 cm layer is the lowest, with most measurements lower than the detection limit of the instrument (Table S-2), which eventually leads to the largest difference in Mo and Cd content in pyrite. Therefore, we believe

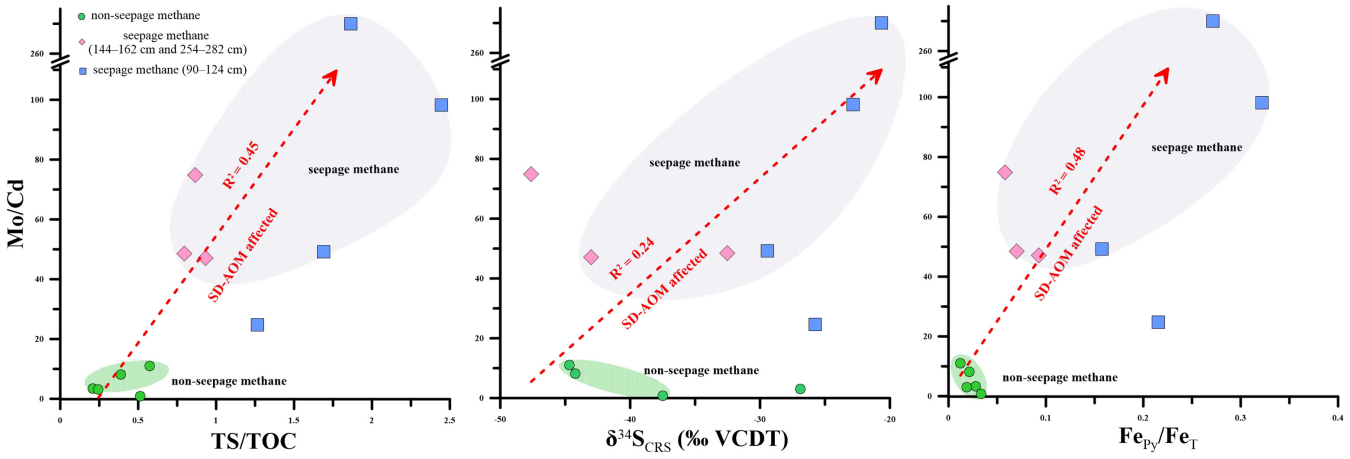

Figure 3 Scatter diagram of Mo/Cd *vs.* TS/TOC, $\delta^{34}S_{CRS}$ and Fe_{Py}/Fe_T (based on Miao *et al.*, 2021a,b). TS/TOC = total sulfur/total organic carbon; CRS = chromium-reducible sulfur; $\delta^{34}S_{CRS}$ = sulfur isotope of chromium-reducible sulfur; Fe_{py} = pyrite Fe; Fe_T = total Fe.

that the chemical composition of diagenetic pyrite has great potential to identify methane seepage.

Acknowledgements

We would like to thank the researchers for the help in the experimental work. And we are also very grateful to Professor J. Peckmann (Universität Hamburg) for his guidance in the writing of this article. This study was supported by the Fundamental Research Funds for the Central Universities (202061007), Key Special Project for Introduced Talents Team of Southern Marine Science and Engineering Guangdong Laboratory (Guangzhou) (GML2019ZD0201), the National Natural Science Foundation of China (41976053), the National Key R&D Program of China (2017YFC0306703).

Editor: Claudine Stirling

Additional Information

Supplementary Information accompanies this letter at http://doi.org/10.7185/geochemlet.2211.

Cite this letter as: Miao, X., Feng, X., Li, J., Liu, X., Liang, J., Feng, J., Xiao, Q., Dan, X., Wei, J. (2022) Enrichment mechanism of trace elements in pyrite under methane seepage. *Geochem. Persp. Let.* 21, 18–22. https://doi.org/10.7185/geochemlet.2211

References

Aharon, P., Fu, B. (2000) Microbial sulfate reduction rates and sulfur and oxygen isotope fractionations at oil and gas seeps in deepwater Gulf of Mexico. *Geochimica et Cosmochimica Acta* 64, 233–246. https://doi.org/10.1016/S0016-7037(99)00292-6

Berner, R.A. (1978) Sulfate reduction and the rate of deposition of marine sediments. *Earth and Planetary Science Letters* 37, 492–498. https://doi.org/10.1016/0012-821X(78)90065-1

Berner, R.A. (1984) Sedimentary pyrite formation: An update. *Geochimica et Cosmochimica Acta* 48, 605–615. https://doi.org/10.1016/0016-7037(84)90089-9

Berner, Z.A., Puchelt, H., Noeltner, T., Kramar, U. (2013) Pyrite geochemistry in the Toarcian Posidonia shale of south-west Germany: evidence for contrasting trace-element patterns of diagenetic and syngenetic pyrites. *Sedimentology* 60, 548–573. https://doi.org/10.1111/j.1365-3091.2012.01350.x

Boetius, A., Ravenschlag, K., Schubert, C.J., Rickert, D., Widdel, F., Gieseke, A., Amann, R., Jørgensen, B., Witte, U., Pfannkuche, O. (2000) A marine microbial consortium apparently mediating anaerobic oxidation of methane. *Nature* 407, 623–626. https://doi.org/10.1038/35036572

Chen, F., Hu, Y., Feng, D., Zhang, X., Cheng, S., Cao, J., Lu, H., Chen, D. (2016) Evidence of intense methane seepages from molybdenum enrichments in gas hydrate-bearing sediments of the northern South China Sea. *Chemical Geology* 443, 173–181. https://doi.org/10.1016/j.chemgeo.2016.09.029

Clark, C., Grguric, B., Schmidt Mumm, A. (2004) Genetic implications of pyrite chemistry from the Palaeoproterozoic Olary Domain and overlying Neoproterozoic Adelaidean sequences, northeastern South Australia. *Ore Geology Reviews* 25, 237–257. https://doi.org/10.1016/j.oregeorev.2004.04.003

Dickens, G.R. (2001) Sulfate profiles and barium fronts in sediment on the Blake Ridge: Present and past methane fluxes through a large gas hydrate reservoir. *Geochimica et Cosmochimica Acta* 65, 529–543. https://doi.org/10.1016/S0016-7037(00)00556-1

Eroglu, S., Scholz, F., Frank, M., Siebert, C. (2020) Influence of particulate versus diffusive molybdenum supply mechanisms on the molybdenum isotope composition of continental margin sediments. *Geochimica et Cosmochimica Acta* 273, 51–69. https://doi.org/10.1016/j.gca.2020.01.009

Huerta-Diaz, M.A., Morse, J.W. (1992) Pyritization of trace metals in anoxic marine sediments. *Geochimica et Cosmochimica Acta* 56, 2681–2702. https://doi.org/10.1016/0016-7037(92)90353-K

Large, R.R., Danyushevsky, L., Hollit, C., Maslennikov, V., Meffre, S., Gilbert, S., Bull, S., Scott, R., Emsbo, P., Thomas, H., Singh, B., Foster, J. (2009) Gold and trace element zonation in pyrite using a laser imaging technique: Implications for the timing of gold in orogenic and carlin-style sediment-hosted deposits. *Economic Geology* 104, 635–668. https://doi.org/10.2113/gsecongeo.104.5.635

Large, R.R., Halpin, J.A., Danyushevsky, L.V., Maslennikov, V.V., Bull, S.W., Long, J.A., Gregory, D.D., Lounejeva, E., Lyons, T.W., Sack, P.J., McGoldrick, P.J., Calver, C.R. (2014) Trace element content of sedimentary pyrite as a new proxy for deep-time ocean atmosphere evolution. *Earth and Planetary Science Letters* 389, 209–220. https://doi.org/10.1016/j.epsl.2013.12.020

Large, R.R., Mukherjee, I., Danyushevsky, L., Gregory, D., Steadman, J., Corkrey, R. (2022) Sedimentary pyrite proxy for atmospheric oxygen; evaluation of strengths and limitations. *Earth-Science Reviews* 227, 103941. https://doi.org/10.1016/j.earscirev.2022.103941

Lin, Z., Sun, X., Peckmann, J., Lu, Y., Xu, L., Strauss, H., Zhou, H., Gong, J., Lu, H., Teichert, B.M.A. (2016) How sulfate-driven anaerobic oxidation of methane affects the sulfur isotopic composition of pyrite: A SIMS study from the South China Sea. *Chemical Geology* 440, 26–41. https://doi.org/10.1016/j.chemgeo.2016.07.007

Miao, X., Feng, X., Li, J., Lin, L. (2021a) Tracing the paleo-methane seepage activity over the past 20,000 years in the sediments of Qiongdongnan Basin, northwestern South China Sea. *Chemical Geology* 559, 119956. https://doi.org/10.1016/j.chemgeo.2020.119956

Miao, X., Feng, X., Liu, X., Li, J., Wei, J. (2021b) Effects of methane seepage activity on the morphology and geochemistry of authigenic pyrite. *Marine and Petroleum Geology* 133, 105231. https://doi.org/10.1016/j.marpetgeo.2021.105231

Morse, J.W., Luther, G. (1999) Chemical influences on trace metal-sulfide interactions in anoxic sediments. *Geochimica et Cosmochimica Acta* 63, 3373–3378. https://doi.org/10.1016/S0016-7037(99)00258-6

Mukherjee, I., Large, R.R. (2020) Co-evolution of trace elements and life in Precambrian oceans: The pyrite edition. *Geology* 48, 1018–1022. https://doi.org/10.1130/G47890.1

Sato, H., Hayashi, K., Ogawa, Y., Kawamura, K. (2012) Geochemistry of deep sea sediments at cold seep sites in the Nankai Trough: insights into the effect of anaerobic oxidation of methane. *Marine Geology* 323, 47–55. https://doi.org/10.1016/j.margeo.2012.07.013

Slotznick, S.P., Eiler, J.M., Fischer, W.W. (2018) The Effects of Metamorphism on Iron Mineralogy and the Iron Speciation Redox Proxy. *Geochimica et Cosmochimica Acta* 224, 96–115. https://doi.org/10.1016/j.gca.2017.12.003

Smrzka, D., Zwicker, J., Bach, W., Feng, D., Himmler, T., Chen, D., Peckmann, J. (2019) The behavior of trace elements in seawater, sedimentary pore water, and their in-corporation into carbonate minerals: A review. *Facies* 65, 1–47. https://doi.org/10.1007/s10347-019-0581-4

Smrzka, D., Feng, D., Himmler, T., Zwicker, J., Hu, Y., Monien, P., Tribovillard, N., Chen, D., Peckmann, J. (2020) Trace elements in methane-seep carbonates: Potentials, limitations, and perspectives. *Earth-Science Reviews* 208, 103263. https://doi.org/10.1016/j.earscirev.2020.103263

Steadman, J.A., Large, R.R., Olin, P.H., Danyushevsky, L.V., Meffre, S., Huston, D., Fabris, A., Lisitsin, V., Wells, T. (2021) Pyrite trace element behavior in magmatic-hydrothermal environments: An LA-ICPMS imaging study. *Ore Geology Reviews* 128, 103878. https://doi.org/10.1016/j.oregeorev.2020.103878

Ulrich, T., Long, D.G.F., Kamber, B.S., Whitehouse, M.J. (2011) In situ trace element and sulfur isotope analysis of pyrite in a Paleoproterozoic gold placer deposit, Pardo and Clement Townships, Ontario, Canada. *Economic Geology* 106, 667–686. https://doi.org/10.2113/econgeo.106.4.667

Wilkin, R.T., Barnes, H.L., Brantley, S.L. (1996) The size distribution of framboidal pyrite in modern sediments: an indicator of redox conditions. *Geochimica et Cosmochimica Acta* 60, 3897–3912. https://doi.org/10.1016/0016-7037(96)00209-8